

Electric field gradients of Lu and Hf in Re

E. Hagn, M. Zahn, and E. Zech

Physik-Department, Technische Universität München, D-8046 Garching, Federal Republic of Germany

(Received 30 December 1982)

The nuclear orientation technique has been applied to dilute ^{173}Lu ($j^\pi=7/2^+$; $T_{1/2}=1.37$ yr) and ^{175}Hf ($j^\pi=5/2^-$; $T_{1/2}=70$ d) nuclei in a hexagonal Re crystal, the activities being produced *in situ* via the nuclear compound reaction $^{185,187}\text{Re}(\alpha, xn\gamma p)$ at $E_\alpha=172.5$ MeV. From the γ -ray anisotropies at temperatures down to 8 mK the quadrupole interaction frequencies $\nu_Q=e^2qQ/h$ of $^{173}\text{LuRe}$ and $^{175}\text{HfRe}$ have been determined as $-1149(100)$ MHz and $-540(43)$ MHz, respectively. The electric field gradients (EFG's) are deduced to be $eq(\text{LuRe})=-13.2(1.2)\times 10^{17}$ V/cm² and $eq(\text{HfRe})=-8.3(8)\times 10^{17}$ V/cm². The negative sign in both cases indicates that the direction of the EFG at the impurity sites is uniquely fixed by the properties of the host lattice. The absolute magnitudes of these EFG's differ strongly from that of the pure system ReRe; they cannot be explained satisfactorily with any correlation known at present.

I. INTRODUCTION

The electric quadrupole interaction of nuclei in noncubic metals has been widely investigated in recent years. From the measured quadrupole interaction energy e^2qQ either the nuclear spectroscopic quadrupole moment Q or the electric field gradient (EFG) eq can be determined if the other corresponding quantity is known. Many experiments have been done for a better understanding of the EFG's in noncubic metals. This is due to the fact that no theoretical model exists with which a large part of the EFG data can be described properly. Only for a few cases of simple nontransition metals has the theoretical description been performed successfully.¹ A review, together with all EFG data through 1980, is given in Refs. 2 and 3. A list of quadrupole frequencies can be found in Ref. 4.

There exist, however, phenomenological models in which the experimental findings are described. Raghavan *et al.*^{5,6} proposed the so-called "universal correlation" between the total EFG, which can be measured, and the lattice gradient, which can be calculated easily using lattice sum methods.^{7,8} With the decomposition of the total EFG eq into an ionic part eq_{ion} and an electronic part eq_{el} ,

$$\begin{aligned} eq &= eq_{\text{ion}} + eq_{\text{el}}, \\ eq_{\text{ion}} &= (1 - \gamma_\infty) eq_{\text{latt}}, \end{aligned} \quad (1)$$

where γ_∞ is the Sternheimer antishielding parameter, this correlation is given by

$$\begin{aligned} eq &= (1 + K)(1 - \gamma_\infty) eq_{\text{latt}}, \\ K &= eq_{\text{el}}/eq_{\text{ion}}, \end{aligned} \quad (2)$$

K being a constant, which was empirically found to be $K \sim -3$. Small deviations due to the individual properties of different impurity-host combinations should be taken into account by a small correction $e\bar{q}$, which is outlined in detail in Ref. 6, the effect of which can also be taken into account by allowing a *small* dependence of K on the special impurity-host combination. According to this correlation all EFG's for hexagonal metals would be expected

to be negative. The positive signs of the EFG's of Gd, Hf, and a few impurity systems were viewed as "glaring exceptions" for which "other sources of the EFG which normally play a secondary role should be of sufficient importance to create strong cancellation effects."⁶

Based on quadrupole interaction nuclear orientation (QINO) measurements on $^{177}\text{LuLu}$, from which a large positive EFG was found, Ernst *et al.*⁹ reexamined the data leading to the universal correlation. They argued that, to a first approximation, the trends of pure systems should be viewed, and impurity systems should be regarded in a second step. They suggested that Eq. (2) holds for *pure systems*, but the proportionality constant K should depend on the atomic group:

$$K \sim -3 \quad \text{for group-IIb, -VIIb, and -VIIIb elements,}$$

$$K \sim +2 \quad \text{for group-IIIb and -IVb elements.}$$

No predictions concerning impurity systems had been made in Ref. 9; especially, the sign of impurity-host systems, one belonging to group IIb, VIIb, or VIIIb and the other to group IIIb or IVb, could not be predicted *a priori*. Subsequent QINO measurements on $^{175}\text{HfLu}$ (group IVb in IIIb, Ref. 10), $^{182}\text{ReLu}$ (group VIIb in IIIb, Ref. 11), and $^{183}\text{OsLu}$ (group VIIIb in IIIb, Ref. 11) led to the proposal that the sign of the EFG is fixed uniquely by the sign of the EFG of the host lattice, independent of the type of the impurity.¹¹ Here we report QINO measurements on inverse systems, namely $^{173}\text{LuRe}$ (group IIIb in VIIb) and $^{175}\text{HfRe}$ (group IVb in VIIIb). The above-mentioned proposal for the sign is again proved, but it will be shown that the absolute magnitude of the EFG depends strongly on the special type of the impurity-host combination, which has the consequence that such systems cannot be described properly by a *universal* correlation of EFG's.

II. NUCLEAR ORIENTATION

The low-temperature nuclear orientation technique (NO) is quite applicable for the measurement of magni-

tude and sign of electric quadrupole splittings. The angular distribution of γ rays emitted in the decay of oriented radioactive nuclei is most conveniently written as¹²

$$W(\theta) = \sum_{k \text{ even}} B_k (h\nu_Q/k_B T) A_k P_k(\cos\theta) Q_k. \quad (3)$$

The parameters B_k describe the degree of orientation; they depend on the spin of the oriented state and on ν_Q/T , where

$$\nu_Q = e^2 q Q / h \quad (4)$$

is the usually quoted quadrupole splitting frequency and T is the temperature of the system. The parameters A_k depend on the characteristics of the nuclear decay; they are products of the usual angular correlation coefficients U_k and F_k , which, e.g., are tabulated in Ref. 13. The $P_k(\cos\theta)$ are Legendre polynomials, θ being the angle between the quantization axis (here the c axis of the single crystal) and the direction of observation. The Q_k in Eq. (3) are solid-angle correction coefficients; they are normally near unity.

In the high-temperature region, $h\nu_Q \ll k_B T$, only the $k=2$ contribution to Eq. (3) plays an essential role, as the orientation parameter B_4 is then much smaller than B_2 . The $B_2(h\nu_Q/k_B T)$ can be expanded in powers of $h\nu_Q/k_B T$, which yields

$$B_2 = -c_j h\nu_Q / k_B T, \quad (5)$$

where c_j is a positive constant depending on the spin j of the oriented state. The γ anisotropy is then given by

$$W(\theta) = 1 - c_j A_2 P_2(\cos\theta) Q_2 \frac{h\nu_Q}{k_B T}, \quad (6)$$

which shows immediately that the magnitude and sign of ν_Q can be determined. Equation (6) shows that it is the product $A_2 \nu_Q$ that can be determined most precisely from a QINO experiment. For an absolute determination of eq a precise value for the product $A_2 Q$ must be available. This information can be obtained from a QINO experiment with the same isotope in a host lattice for which the EFG is known. The ratio of the corresponding γ anisotropies yields the ratio of the EFG's:

$$\frac{W^{(1)}(\theta) - 1}{W^{(2)}(\theta) - 1} = \frac{(A_2 e^2 q Q)^{(1)}}{(A_2 e^2 q Q)^{(2)}} = \frac{eq^{(1)}}{eq^{(2)}}. \quad (7)$$

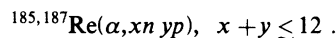
This means that a detailed knowledge of the single quantities A_2 and Q is not necessary. Equation (7) holds exactly for the high-temperature range, where the $k=4$ terms can be neglected and the linear dependence of B_2 on $h\nu_Q/k_B T$ is a good approximation. For lower temperatures, where the latter conditions are not fulfilled, the ratio $eq^{(1)}/eq^{(2)}$ can be determined as a function of the nuclear parameters. It is found that this ratio remains nearly constant, at least for reasonable variations of the nuclear parameters, thus allowing a precise determination of the ratios of EFG's.

III. SAMPLE PREPARATION AND EXPERIMENTAL DETAILS

The first attempts to prepare dilute alloys of group-IIIb and -IVb elements in group-IIb, -VIIb, and -VIIIb hexagonal crystals were performed by 20-kV mass-separator im-

plantation of ^{177}Lu ($j^\pi=7/2^+$, $T_{1/2}=6.7$ d) into single crystals of Lu, Re, and Os. As the γ anisotropy of the mass-separator-implanted $^{177}\text{LuLu}$ sample was found to be much smaller than the γ anisotropy of a $^{177}\text{LuLu}$ sample, the activity being prepared *in situ* via the (n,γ) nuclear reaction, it was concluded that the quadrupole splittings measured for $^{177}\text{LuRe}$ and $^{177}\text{LuOs}$ did not represent the correct bulk-material value.¹⁴ Therefore, keeping in mind that the nuclear orientation technique is not restricted to special isotopes (in principle, each radioactive isotope with $j \geq 1$ and a sufficiently long half-life is suitable), an *in situ* preparation with an appropriate nuclear reaction was viewed more promising.

A sample that contained activities of ^{173}Lu ($j^\pi=7/2^+$, $T_{1/2}=1.37$ yr) and ^{175}Hf ($j^\pi=5/2^-$, $T_{1/2}=70$ d) was prepared in the following way: From a rhenium single-crystal rod, purchased from MRC, a disk with about 6 mm diameter and a thickness of ~ 0.2 mm was spark-cut. The crystal c axis was oriented perpendicularly to the disk plane, the accuracy of the orientation being $\sim 1^\circ$. The surfaces of the crystal were mechanically and electrolytically polished. This crystal was irradiated with 172.5-MeV α particles for 30 min with a mean current of 4 μA at the cyclotron in Jülich. At this beam energy the following nuclear compound reactions take place:



(In principle, for the production of proton-deficient nuclei, irradiation with protons or deuterons would be more favorable; p or d beams with a sufficiently high energy were, however, not easily available.) After the short-lived activities had been allowed to decay for 2 weeks, the crystal was annealed at $T \sim 2000^\circ\text{C}$ for 2 h in vacuum ($< 10^{-6}$ Torr). It was then ultrasonically soldered to the cold finger of an adiabatic demagnetization cryostat, the details of which are described in Ref. 15. For thermometry a $^{60}\text{CoCo}(\text{hcp})$ single-crystal sample (c axis perpendicular to the disk plane) was GaIn-soldered to the other side of the cold finger. With CrK alum as the cooling salt the sources were cooled to a final temperature of ~ 11 mK. An external magnetic field of 1 kG was applied to establish a good thermal conductivity of the soldered joints. During two warm-up periods from 11 to ~ 20 mK γ -ray spectra were measured with two coaxial Ge(Li) detectors that were placed at 0° and 90° with respect to the c axes of the single crystals. Every 1000 seconds the spectra were recorded onto magnetic tape. For normalization, spectra were measured before and after the cold periods. The final analysis was done with a Digital Equipment Corporation PDP11/45 computer. The peak intensities were determined with least-squares fits assuming a Gaussian line shape with an exponential tail and a background that was constant, linear, quadratic, and error-function-like.¹⁶

After a further decay period of 9 weeks a second experiment was performed, first, to improve statistical accuracy, and second, in order to check whether temperature gradients were present between the cold finger and the Re crystal. In this experiment a lower final temperature of 8 mK was obtained because of the smaller radioactive heating, and a temperature gradient, if present, should have been smaller. Both experiments yielded consistent results, however, thus excluding the existence of a temperature difference between the Re crystal and the $^{60}\text{CoCo}(\text{hcp})$

thermometer. (Because of the known good soldering properties of Co a temperature gradient between the cold finger and the Co thermometer can be excluded.)

Figure 1 shows a γ -ray spectrum measured at the beginning of the second experiment. The assignment of the γ -ray lines to the corresponding isotope was performed with two independent methods: first, via the γ -ray energy, which could be determined to $\sim \pm 0.2$ keV (the γ -ray energies of all isotopes are tabulated in Ref. 17), and second, via the half-life connected with the different γ -ray lines. (The half-lives were determined by analyzing the time dependence of the γ -ray intensities of "warm" spectra measured before and after the demagnetizations and, for long-lived isotopes, of "warm" spectra measured over a period of several months.) In addition to the γ -ray lines arising from the decays of ^{173}Lu ($E=272$ keV) and ^{175}Hf ($E=343$ keV) there are many γ -ray lines originating from isotopes of which the quadrupole splitting in Re has been known, e.g., ^{183}Re and ^{184}Re . The corresponding γ anisotropies were also analyzed. All errors quoted for our results include, in addition to the statistical error, a systematic error, which has been estimated from the reproducibility of our QINO measurements.

IV. RESULTS

A. $^{173}\text{LuRe}$

A simplified decay scheme of ^{173}Lu is illustrated in Fig. 2. Only the 272-keV γ -ray line could be detected in both experiments with moderate statistical accuracy. [The 79-keV γ rays are strongly absorbed by the cryostat. At $E \sim 100$ keV several γ -ray lines were present, originating from other isotopes. In spectra that were accumulated for 2 d the 171-keV transition could be resolved with the correct ratio of intensities $I(173)/I(272)=0.14$ (Ref. 17).] Figure 3 shows the γ anisotropy of the 272-keV transition versus $1/T$. The A_k coefficients are known experimentally from "magnetic" NO measurements on ^{173}Lu in ZrFe_2 : $A_2 = -0.25(2)$ and $A_4 = 0.0(2)$.¹⁸ Taking these values into account, the least-squares fit yields (in MHz)

$$v_Q(^{173}\text{LuRe}) = -1149(100).$$

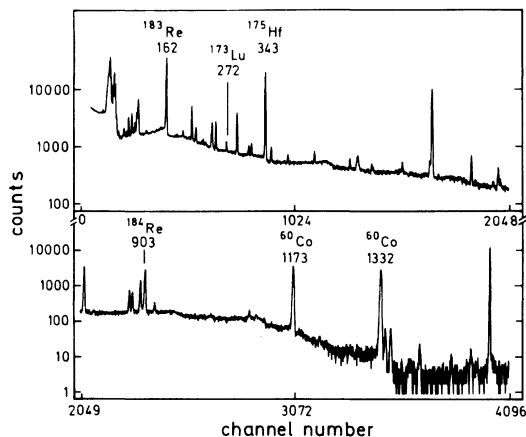


FIG. 1. γ -ray spectrum measured at the beginning of the second experiment (11 weeks after the irradiation).

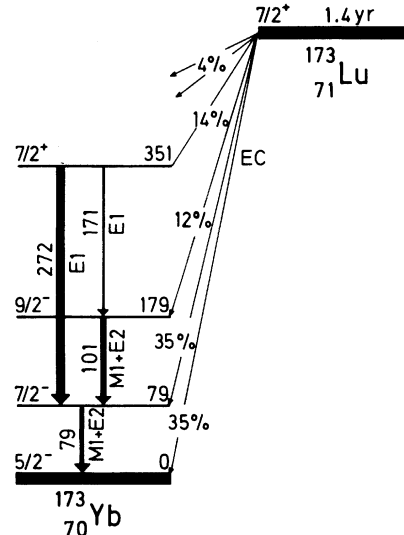


FIG. 2. Simplified decay scheme of ^{173}Lu .

The solid line in Fig. 3 represents the corresponding theoretical curve.

B. $^{175}\text{HfRe}$

In the decay of ^{175}Hf (see Fig. 4) one strong γ transition with an energy of 343 keV takes place (absolute intensity 86.9%). The γ anisotropy is shown in Fig. 5. As outlined in detail in Sec. II, it is the product $A_2 v_Q$ that can be determined most precisely from QINO measurements. The solid line in Fig. 5 represents the result of a least-squares fit utilizing Eq. (3), from which

$$A_2 v_Q(^{175}\text{HfRe}) = +83.7(3.0)$$

is obtained (in MHz), taking into account realistic estimates for A_4 according to the decay properties of ^{175}Hf [$\delta(343) = -0.26(3)$ (Ref. 19); the tensor rank of the β transition to the 343-keV level is $L=1$ with admixtures of $L=0$ and $L=2$ components]. It should be noted that the

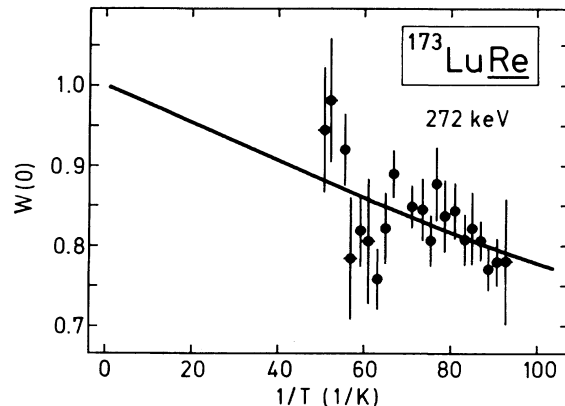
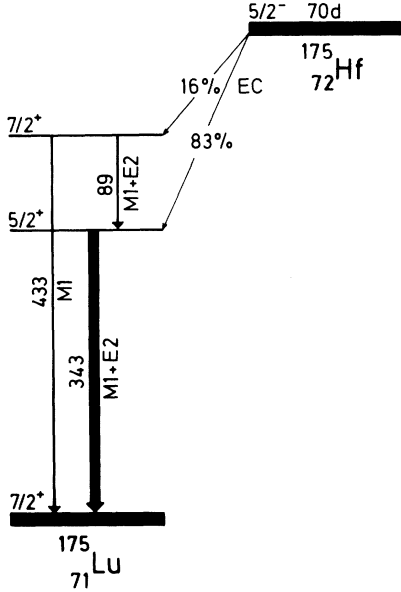


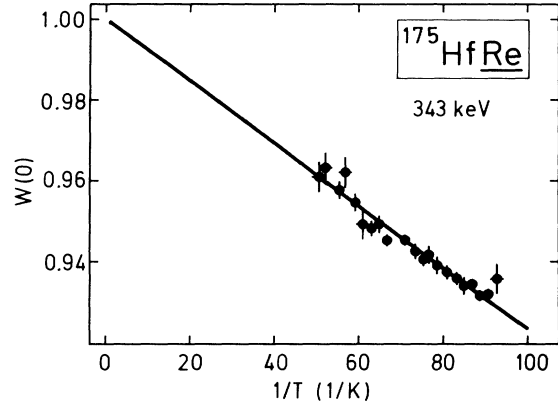
FIG. 3. $^{173}\text{LuRe}$ γ anisotropy of the 272-keV transition measured at $\theta=0^\circ$ versus $1/T$.

FIG. 4. Simplified decay scheme of ^{175}Hf .

uncertainty due to the unknown β -decay matrix elements via the $k=4$ term in Eq. (3) is negligibly small. As the A_2 coefficient is known from “magnetic” NO measurements of ^{175}Hf in ZrFe_2 only imprecisely because of a small γ anisotropy, $A_2 = -0.169(24)$ (Ref. 20), we use the results of a QINO measurement on $^{175}\text{HfHf}$ by Kaindl *et al.*²¹ for further analysis. In Ref. 21 only the result for ν_Q is quoted [$\nu_Q = 980(100)$ MHz], the error being relatively large because of the uncertainty of A_2 . The product $A_2\nu_Q$ is, however, again more precise. Taking into account the data of Ref. 21, we derive $A_2\nu_Q(^{175}\text{HfHf}) = -94.7(5.0)$ MHz. The larger error in this quantity is partly due to the fact that the linear dependence of B_2 on ν_Q of Eq. (5) is a worse approximation for positive ν_Q than for negative ν_Q . (This is due to a partial cancellation of higher-order contributions in the Taylor series, which depends on the sign of ν_Q .) The ratio of EFG’s is now given by the ratio of $A_2\nu_Q$:

$$\frac{A_2\nu_Q(^{175}\text{HfRe})}{A_2\nu_Q(^{175}\text{HfHf})} = \frac{eq(^{175}\text{HfRe})}{eq(^{175}\text{HfHf})} = -0.88(8).$$

The EFG of HfHf can be deduced from a Mössbauer effect measurement on the 2^+ state of ^{178}Hf in Hf . With $\nu_Q(^{178}\text{HfHf}) = -443(15)$ MHz (Ref. 22) and $Q^{(2^+)}(^{178}\text{Hf}) = -1.95(2)$ b (Ref. 23) one gets $eq(\text{HfHf}) = +9.38(32) \times 10^{17}$ V/cm². With these data the EFG of HfRe is now deduced to be

FIG. 5. $^{175}\text{HfRe}$ γ anisotropy of the 343-keV transition measured at $\theta=0^\circ$ vs $1/T$.

$$eq(\text{HfRe}) = -8.3(8) \times 10^{17}$$

in V/cm².

C. Other isotopes

As can be seen from the γ -ray spectrum of Fig. 1 several other isotopes were produced in the $^{185,187}\text{Re}(\alpha, xn\gamma p)$ reaction. The corresponding quadrupole splittings are listed in Table I. The results for $^{182m}\text{ReRe}$ and $^{178}\text{TaRe}$ yield, taking into account the known EFG’s, quadrupole moments that agree well with predictions from the rotational model. (These quadrupole splittings were not known before.) The results for $^{183,184}\text{ReRe}$ agree within 1 standard deviation with the experimental values of Ref. 24 (column 5 in Table I). The quadrupole splitting of $^{186}\text{ReRe}$ is smaller than that of Ref. 24, but agrees with the expectation, taking into account the ratio of quadrupole moments $Q(^{186}\text{Re})/Q(^{185}\text{Re})$ measured recently by optical hyperfine spectroscopy.²⁵

V. DISCUSSION

As the quadrupole splittings measured for ^{178}Ta and $^{182m,183,184,186}\text{Re}$ agree well with either the expectation from a nuclear physics point of view or with data already known, we conclude that the quadrupole splittings derived for $^{173}\text{LuRe}$ and $^{175}\text{HfRe}$ can reliably be used to derive the corresponding EFG’s.

In the case of ^{173}Lu the quadrupole moment is not known experimentally. A precise estimate is obtained in the following way: It is well known that the ground states of $^{173,175,177}\text{Lu}$ can be described by a $j^\pi K(Nn_z\Lambda)$

TABLE I. Electric quadrupole splittings in Re.

Isotope	j^π	$T_{1/2}$	ν_Q (MHz)	ν_Q (MHz) (Ref. 24)
^{178}Ta	1^+	9.3 min	-103(10)	
^{182m}Re	7^+	64 h	-502(30)	
^{183}Re	$5/2^+$	71 d	-281(20)	-262(24)
^{184}Re	3^-	38 d	-340(22)	-390(33)
^{186}Re	1^-	90.6 h	-73(7)	-104(14)

$= 7/2 + 7/2$ [404] Nilsson configuration (Ref. 26 and references therein). For stable ^{175}Lu the spectroscopic ground-state quadrupole moment is known from muonic x-ray spectroscopy to be $Q = +3.49(2)$ b.²⁷ For ^{175}Lu and ^{177}Lu optical hyperfine spectroscopy data are available.^{28,29} With the ratio $B(^{177}\text{Lu})/B(^{175}\text{Lu}) = 0.97051(8)$ the ground-state spectroscopic quadrupole moment of ^{177}Lu is calculated to be $Q = +3.39(2)$ b. The extrapolation to ^{173}Lu leads to $Q(^{173}\text{Lu}) = +3.6(1)$ b, the error being adjusted sufficiently large that the uncertainty due to the different nuclear deformations of these isotopes is taken into account. All these quadrupole moments agree well with the expectation for a rigid rotator,

$$Q = Q_0 \frac{j(2j-1)}{(j+1)(2j+3)}, \quad (8)$$

where Q_0 is the intrinsic quadrupole moment known from, e.g., $B(E2)$ transition probabilities.^{23,30} Taking now $Q(^{173}\text{Lu}) = +3.6(1)$ b, we find

$$eq(\text{LuRe}) = -13.2(1.2) \times 10^{17}$$

in units of V/cm^2 .

For ^{175}Hf a precise knowledge of the quadrupole moment is not necessary to derive the EFG, as was shown in Sec. IV B. Here we want to mention that the quadrupole moment of ^{175}Hf derived in Ref. 21, $Q = +2.7(4)$ b, is also in good agreement with the expectation.

In Table II the quadrupole splittings of a series of elements as impurities in Lu and Re are compiled, together with most recent data for the quadrupole moments of the states involved. (Some of these quadrupole moments differ seriously from the usual tabular values as, e.g., given in Ref. 4.) All EFG's that are listed in column 5 of Table II, follow the sign rule of Ref. 11: The sign of the EFG is fixed uniquely by the host lattice. The absolute magnitudes, however, show considerable variations. This can be seen in Fig. 6, where the total EFG's are plotted as function of Z , where Z is the number of outer electrons of

TABLE II. Electric quadrupole splittings and EFG's in Lu and Re host lattices.

System	j^π	Q (b)	ν_Q (MHz)	eq (10^{17} V/cm ²)
$^{177}\text{LuLu}$	$7/2^+$	$+3.39(2)^a$	$+294(37)^m$	$+3.6(5)$
$^{175}\text{HfLu}$	$5/2^-$	$+2.7(4)^b$	$+364(24)^n$	$+5.6(9)$
$^{181}\text{TaLu}$	$5/2^+$	$+2.35(6)^c$	$302.8(1.6)^o$	$(+)5.33(14)$
$^{182}\text{ReLu}$	2^+	$+1.8(2)^d$	$+311(24)^n$	$+6.6(6)$
$^{183}\text{OsLu}$	$9/2^+$	$+2.8(4)^e$	$+403(20)^n$	$+6.0(6)$
$^{193}\text{IrLu}$	$3/2^+$	$+0.78(3)^f$	$281(3)^p$	$(+)14.9(6)$
$^{197}\text{AuLu}$	$3/2^+$	$+0.547(16)^g$	$+300(3)^q$	$+22.7(7)$
$^{173}\text{LuRe}$	$7/2^+$	$+3.6(1)^h$	$-1149(100)^r$	$-13.2(1.2)$
$^{175}\text{HfRe}$	$5/2^-$	$+2.7(4)^b$	$-540(43)^r$	$-8.3(8)^w$
$^{181}\text{TaRe}$	$7/2^+$	$+3.28(6)^i$	$-520(5)^s$	$-6.56(14)$
$^{187}\text{ReRe}$	$5/2^+$	$+2.09(4)^i$	$-255.2(5)^t$	$-5.05(5)$
$^{186}\text{OsRe}$	2^+	$-1.63(3)^k$	$+151(13)^u$	$-3.83(34)$
$^{193}\text{IrRe}$	$3/2^+$	$+0.78(3)^f$	$-76(7)^q$	$-4.0(4)$
$^{197}\text{AuRe}$	$3/2^+$	$+0.547(16)^g$	$-43(17)^q$	$-3.3(1.3)$
$^{197m}\text{HgRe}$	$13/2^+$	$+1.47(13)^l$	$-110(15)^v$	$-3.1(5)$

^aRecalculated with the data of Refs. 27–29; see also text.

^bReference 21.

^cRecalculated with $\nu_Q^{(5/2^+)}(^{181}\text{TaRe}) = (-)372(4)$ MHz (Ref. 31), $\nu_Q^{(7/2^+)}(^{181}\text{TaRe}) = -520(5)$ MHz (Ref. 32), and $Q^{(7/2^+)} = +3.28(6)$ b (Ref. 33).

^dReference 24; recalculated with $eq(\text{ReRe}) = -5.05(5) \times 10^{17}$ V/cm² (see row 11) instead of $-4.87(15) \times 10^{17}$ V/cm².

^eReference 34.

^fReference 35.

^gReference 36.

^hSee text.

ⁱReference 33.

^kAverage value; see Ref. 37.

^lReference 38.

^mReference 9.

ⁿReference 11.

^oReference 41.

^pReference 39.

^qReference 40; value quoted in Ref. 4.

^rThis work.

^sReference 32.

^tReference 42.

^uReference 43.

^vReference 44.

^wDeduced from the ratio $eq(\text{HfRe})/eq(\text{HfHf})$; see text.

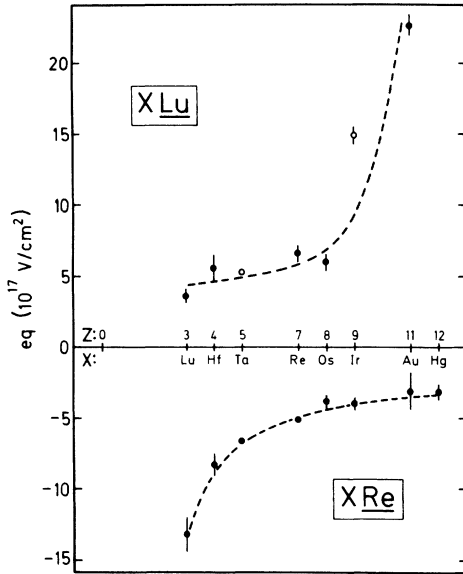


FIG. 6. Total EFG's eq of different impurities in Lu (top) and Re (bottom) vs Z , where Z is the number of "outer" electrons. Open circles represent data for which the sign is not known experimentally. For these cases the sign is predicted. The dashed curves indicate the trend.

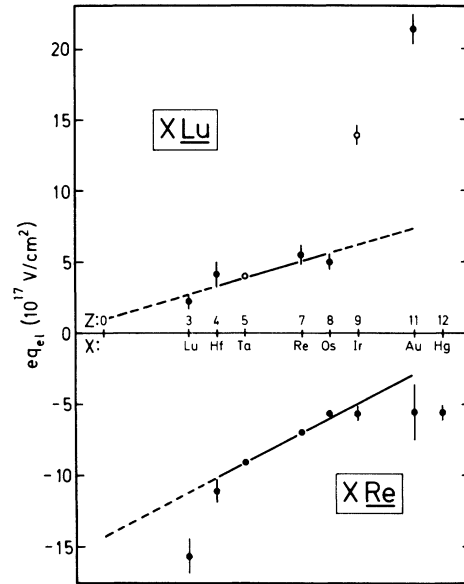


FIG. 7. Electronic contribution eq_{el} to the EFG for different impurities in Lu (top) and Re (bottom). Open circles represent data for which eq_{el} has been deduced from EFG's, the sign of which is not known experimentally. The solid lines are results from least-squares fits assuming a linear dependence on Z , where Z is the number of "outer" electrons of the impurity atoms.

the impurity atoms. The dashed curves indicate the trend.

A decomposition of the total EFG's into the ionic and electronic contributions, $eq_{ion} = (1 - \gamma_{\infty})eq_{latt}$ and eq_{el} , respectively, is given in Table III. Here the lattice gradients eq_{latt} have been calculated with the known lattice parameters of Lu and Re (Ref. 45) and the Sternheimer factors have been taken from Refs. 46–48. The systematic behavior of eq_{el} and the ratio $K = eq_{el}/eq_{ion}$ is illustrated in Figs. 7 and 8. The following discussion is given separately for the cases Lu and Re as the host lattice.

A. XLu

The electronic contribution eq_{el} for different impurities in Lu (upper part of Fig. 7) for $3 \leq Z \leq 8$ seems to be linearly dependent on Z . A least-squares fit yields $eq_{el}(Z=0) = 1.0(8) \times 10^{17} \text{ V/cm}^2$ and $d(eq_{el})/dZ = +0.6(2) \times 10^{17} \text{ V/cm}^2$ (solid line in Fig. 7). Such a dependence could be understood, as in a naive model the electronic field gradient should be proportional to the

TABLE III. Total EFG eq ionic and electronic contributions, eq_{ion} and eq_{el} , respectively, the ratio K of electronic to ionic contribution for different impurities in Lu and Re host lattices. The field gradients are given in units of 10^{17} V/cm^2 .

System	eq	$1 - \gamma_{\infty}$	eq_{ion}	eq_{el}	K
LuLu	+ 3.6(5)	62	+ 1.36	+ 2.2(5)	1.6(4)
HfLu	+ 5.6(9)	69	+ 1.51	+ 4.1(9)	2.7(6)
TaLu	(+)5.33(14)	62	+ 1.36	[+ 4.0(2)]	2.9(2)
ReLu	+ 6.6(6)	45–51	+ 1.1(1)	+ 5.5(7)	5.0(8)
OsLu	+ 6.0(6)	47	+ 1.02	+ 5.0(6)	4.9(6)
IrLu	(+)14.9(6)	41–44	+ 1.0(1)	[+ 13.9(7)]	13.9(1.6)
AuLu	+ 22.7(7)	39–73	+ 1.3(4)	+ 21.4(1.1)	16.5(5.1)
LuRe	– 13.2(1.2)	62	+ 2.54	– 15.7(1.2)	– 6.2(5)
HfRe	– 8.3(8)	69	+ 2.81	– 11.1(8)	– 4.0(3)
TaRe	– 6.56(14)	62	+ 2.54	– 9.1(2)	– 3.6(1)
ReRe	– 5.05(5)	45–51	+ 1.9(2)	– 7.0(2)	– 3.7(4)
OsRe	– 3.8(3)	47	+ 1.91	– 5.7(3)	– 3.0(2)
IrRe	– 4.0(4)	41–44	+ 1.7(1)	– 5.7(5)	– 3.4(4)
AuRe	– 3.3(1.3)	39–73	+ 2.3(7)	– 5.6(2.0)	– 2.4(1.1)
HgRe	– 3.1(5)	61	+ 2.49	– 5.6(5)	– 2.2(2)

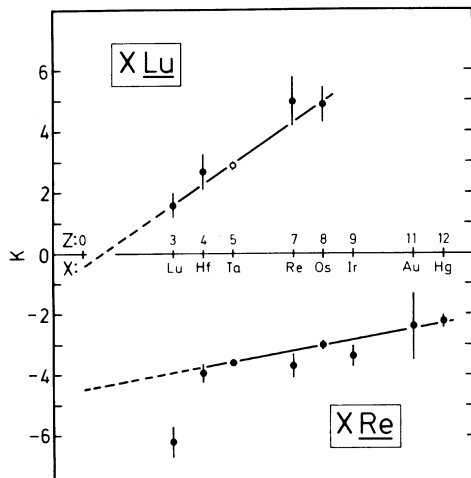


FIG. 8. Ratio $K = eq_{el}/eq_{ion}$ of electronic to ionic contributions to the total EFG for different impurities in Lu (top) and Re (bottom) vs Z , where Z is the number of the "outer" electrons of the impurity atoms. The solid lines are the results of least-squares fits, assuming a linear dependence on Z .

number of electrons producing this gradient, i.e., the number of "outer" electrons. The electronic field gradients for $IrLu$ and $AuLu$ are much larger than expected from the extrapolation, assuming the linear dependence on Z , as can be seen from Fig. 7. At present we cannot state if the EFG data for $IrLu$ (Ref. 39) and $AuLu$ (Refs. 40 and 4) actually represent the "dilute-impurity" value, as both alloys were prepared by melting, and reliable metallurgical data for the solubility of Ir and Au in Lu are not available. (It could be possible that intermetallic compounds are formed in the melting steps for which the EFG may be quite different from that of a "dilute-impurity" sample.)

For the proportionality constant K between eq_{el} and eq_{ion} the data are also consistent with a linear dependence on Z , as can be seen in the upper part of Fig. 8. Here the data for $IrLu$ and $AuLu$ have been omitted because of the reasons mentioned before. A least-squares fit yields $K(Z=0) = -0.4(6)$ and $dK/dZ = 0.68(13)$.

A similar linear behavior of K with the impurity valence Z' has been observed for different impurities in a Zn matrix.^{49,50} (The discrepancy for $HgZn$, which was due to an erroneous quadrupole moment used for the derivation of the EFG, has been removed now.^{50,51}) Recent measurements of the EFG of $AgZn$ by van Walle *et al.*⁵² support the linear dependence of K on Z also. Thus one could get the impression that a linear increase of the electronic field gradient with Z could be a general effect. The data of XRe that are discussed in the following section contradict this assumption.

B. XRe

The electronic field gradients for different impurities in Re are shown in the lower part of Fig. 7. Here the behavior is different: The absolute value of eq_{el} decreases with increasing Z , which cannot be understood in terms of the above-mentioned model of an electronic field gradient

proportional to the number of "outer" electrons, according to which the opposite behavior would be expected. For $4 \leq Z \leq 8, \dots, 11$ the data are consistent with a linear decrease of $|eq_{el}|$ as a function of Z . Taking into account the data for $4 \leq Z \leq 11$, a least-squares fit yields $eq_{el}(Z=0) = 14.2(8) \times 10^{17}$ V/cm² and $d|eq_{el}|/dZ = -1.0(1) \times 10^{17}$ V/cm². Thus one could get the impression that eq_{el} now depends (almost linearly) on the number of missing electrons or electron holes.

The almost constant electronic field gradient for $8 \leq Z \leq 12$ might, in principle, be understandable, because the number of "outer" electrons is clearly different from the valence of the impurity atoms, and s -wave-like electrons will not give a contribution to eq_{el} . On the other hand, the concept of a pure valence as, e.g., used by Raghavan *et al.*,⁶ according to which $Z'=4$ would be expected for Hf and Os, is ruled out by the present data, as eq_{el} differs by a factor of ~ 2 for $HfRe$ and $OsRe$.

The dependence of $K(XRe)$ on Z is shown in Fig. 8. The data for $4 \leq Z \leq 12$ are again consistent with a linear dependence of K on Z , with parameters $K(Z=0) = -4.4(3)$ and $d|K|/dZ = -0.18(5)$. The absolute value of the ratio of electronic and ionic field gradients decreases with increasing Z . Raghavan and Raghavan⁵³ proposed a refined correlation between the electronic and ionic field gradients, according to which K should be constant for impurities with the same nominal valence; our experimental data contradict this proposal.

For $LuRe$ the absolute magnitudes of the electronic field gradient and hence also of K are much larger than expected from the systematics. Metallurgical problems cannot be the origin, as the $LuRe$ sample has been prepared *in situ* with a nuclear reaction, the concentration of Lu being below the ppm level. On the other hand, we cannot exclude that Lu may occupy interstitial lattice sites in the Re single crystal, as the atomic radii are strongly different. In this case a non-axially-symmetric field gradient could act on the impurity nuclei, depending on the type of the interstitial sites. Such a situation can be detected with nuclear orientation on an isotope in the decay where $L=1$ and $L=2$ γ transitions take place via the observable fact that a nonaxiality of the EFG causes the ratio of the 0° and 90° anisotropies to be different for γ transitions with different multiplicities, the decisive parameter being the ratio of A_k coefficients, i.e., A_4/A_2 . In the present case this feature could not be utilized; only one γ transition could be measured with reasonable accuracy, which, in addition, had a vanishing A_4 coefficient.

VI. CONCLUSIONS

Our experiments have shown that the *in situ* preparation of radioactive impurities in hexagonal single crystals is a good technique to produce highly dilute samples well suited for the systematic study of the quadrupole interaction in noncubic metals. Elements with a proton number smaller than that of the single-crystal target can be produced by bombardment with light particles at high energies. The use of high-energy protons will probably allow the production of impurity-host combinations that are hardly accessible with other techniques.

The EFG's deduced in the present work together with data from other measurements show some systematic behavior: (1) The sign of the EFG is fixed uniquely by the properties of the host. (2) For chains of different impurities in the same host lattice there is a smooth variation of the electronic field gradient; within some limits (which cannot be specified precisely at present) there seems to be a linear dependence of eq_{el} and/or eq_{el}/eq_{ion} on the electron number of the impurities. (3) There is no "universal" correlation describing the experimentally known EFG data in detail.

ACKNOWLEDGMENT

We are indebted to Professor P. Kienle for his kind interest and continuous support of this work. We also wish to thank Dr. P. Jahn and the Jülich cyclotron crew for performing the irradiation. Experimental help by E. Smolic and H. Kleebauer is acknowledged. This work was supported by the Bundesministerium für Forschung und Technologie, Bonn, and, in part, by the Kernforschungszentrum, Jülich.

- ¹T. P. Das, Phys. Scr. **11**, 121 (1975).
- ²E. N. Kaufmann and R. J. Vianden, Rev. Mod. Phys. **51**, 161 (1979).
- ³E. N. Kaufmann, Hyperfine Interact. **9**, 219 (1981).
- ⁴R. Vianden, Hyperfine Interact. **10**, 1243 (1981).
- ⁵R. S. Raghavan, E. N. Kaufmann, and P. Raghavan, Phys. Rev. Lett. **34**, 1280 (1975).
- ⁶P. Raghavan, E. N. Kaufmann, R. S. Raghavan, E. J. Ansaldo, and R. A. Naumann, Phys. Rev. B **13**, 2835 (1976).
- ⁷F. W. de Wette, Phys. Rev. **123**, 103 (1961).
- ⁸T. P. Das and M. Pomerantz, Phys. Rev. **123**, 2070 (1961).
- ⁹H. Ernst, E. Hagn, E. Zech, and G. Eska, Phys. Rev. B **19**, 4460 (1979).
- ¹⁰H. Ernst, E. Hagn, and E. Zech, J. Phys. F **9**, 1701 (1979).
- ¹¹H. Ernst, E. Hagn, and E. Zech, Phys. Rev. B **22**, 2248 (1980).
- ¹²S. R. de Groot, H. A. Tolhoek, and W. J. Huiskamp, in *Alpha-, Beta- and Gamma-Ray Spectroscopy*, edited by K. Siegbahn (North-Holland, Amsterdam, 1968), Vol. 2, p. 1199ff.
- ¹³T. Yamazaki, Nucl. Data **A3**, 1 (1967).
- ¹⁴Christine Trautmann, diploma thesis, Technische Universität München, 1980 (unpublished).
- ¹⁵E. Hagn, K. Leuthold, E. Zech, and H. Ernst, Z. Phys. A **295**, 385 (1980).
- ¹⁶M. Dojo, Nucl. Instrum. **115**, 425 (1974).
- ¹⁷G. Erdtmann and W. Soyka, in *Topical Presentations in Nuclear Chemistry*, edited by K. H. Lieser (Verlag Chemie, Weinheim, 1979), Vol. 7.
- ¹⁸K. S. Krane, C. E. Olsen, S. S. Rosenblum, and W. A. Steyert, Phys. Rev. C **12**, 1999 (1975).
- ¹⁹P. Erman, B. I. Deutch, and C. J. Herrlander, Nucl. Phys. **A92**, 241 (1967).
- ²⁰K. S. Krane, S. S. Rosenblum, and W. A. Steyert, Phys. Rev. C **14**, 656 (1976).
- ²¹G. Kaindl, F. Bacon, and J. A. Soinski, Phys. Lett. **46B**, 62 (1973).
- ²²P. Boolchand, B. L. Robinson, and S. Jha, Phys. Rev. **187**, 475 (1969).
- ²³K. E. G. Löbner, M. Vetter, and V. Höning, Nucl. Data Tables **A7**, 495 (1970).
- ²⁴H. Ernst, E. Hagn, and E. Zech, Phys. Rev. C **23**, 1739 (1981).
- ²⁵S. Büttgenbach, R. Dicke, G. Götz, and F. Träber, Z. Phys. A **302**, 281 (1981).
- ²⁶*Tables of Isotopes*, 7th ed., edited by C. M. Lederer and V. S. Shirley (Wiley, New York, 1978).
- ²⁷W. Dey, P. Ebersold, H. J. Leisi, F. Scheck, H. K. Walter, and A. Zehnder, Nucl. Phys. **A326**, 418 (1979).
- ²⁸G. J. Ritter, Phys. Rev. **126**, 240 (1962).
- ²⁹F. R. Petersen and H. A. Shugart, Phys. Rev. **126**, 252 (1962).
- ³⁰P. Möller and J. R. Nix, At. Data Nucl. Data Tables **26**, 165 (1981).
- ³¹G. Netz and E. Bodenstedt, Nucl. Phys. **A208**, 503 (1973).
- ³²G. Kaindl, D. Salomon, and G. Wortmann, Phys. Rev. Lett. **28**, 952 (1972).
- ³³J. Konijn, W. van Doesburg, G. T. Ewan, T. Johansson, and G. Tibell, Nucl. Phys. **A360**, 187 (1981).
- ³⁴E. Hagn, H. Kleebauer, and E. Zech, Phys. Lett. **104B**, 365 (1981).
- ³⁵L. A. Schaller and W. Dey, Helv. Phys. Acta **47**, 482 (1974).
- ³⁶R. J. Powers, P. Martin, G. H. Miller, R. E. Welsh, and D. A. Jenkins, Nucl. Phys. **A230**, 413 (1974).
- ³⁷H. Ernst, E. Hagn, and E. Zech, Nucl. Phys. **A332**, 41 (1979).
- ³⁸G. Huber, J. Bonn, H.-J. Kluge, and E. W. Otten, Z. Phys. A **276**, 187 (1976); J. Bonn, G. Huber, H.-J. Kluge, and E. W. Otten, *ibid.* **276**, 203 (1976).
- ³⁹M. Forker and K. Krusch, Phys. Rev. B **21**, 2090 (1980).
- ⁴⁰G. Wortmann, B. Perscheid, G. Kaindl, and F. E. Wagner, Hyperfine Interact. **9**, 343 (1981).
- ⁴¹T. Butz and W. Potzel, Hyperfine Interact. **1**, 157 (1975).
- ⁴²M. Stachel and H. E. Bömmel, Appl. Phys. A **30**, 27 (1983).
- ⁴³H. Ernst, W. Koch, F. E. Wagner, and E. Bucher, Phys. Lett. **70A**, 246 (1979).
- ⁴⁴P. Herzog, K. Krien, J. C. Soares, H. R. Folle, K. Freitag, F. Reuschenbach, M. Reuschenbach, and R. Trzcinski, Phys. Lett. **66A**, 495 (1978).
- ⁴⁵W. B. Pearson, *A Handbook of Lattice Spacings and Structures of Metals and Alloys* (Pergamon, London, 1967), Vol. 2, p. 80.
- ⁴⁶F. D. Feiock and W. R. Johnson, Phys. Rev. **187**, 39 (1969).
- ⁴⁷R. P. Gupta and S. K. Sen, Phys. Rev. A **7**, 850 (1973).
- ⁴⁸R. P. Gupta and S. K. Sen, Phys. Rev. A **8**, 1169 (1973).
- ⁴⁹J. C. Soares, K. Krien, P. Herzog, H.-R. Folle, K. Freitag, F. Reuschenbach, M. Reuschenbach, and R. Trzcinski, Z. Phys. B **31**, 395 (1978).
- ⁵⁰K. Krien, F. Reuschenbach, J. C. Soares, R. Vianden, R. Trzcinski, K. Freitag, M. Hage-Ali, and P. Siffert, Hyperfine Interact. **7**, 413 (1980).
- ⁵¹P. Herzog, K. Krien, K. Freitag, M. Reuschenbach, and H. Walitzki, Nucl. Phys. **A337**, 261 (1980).
- ⁵²E. van Walle, D. Vandeplassche, C. Nuytten, J. Wouters, and L. Vanneste, Phys. Rev. B **28**, 1109 (1983).
- ⁵³R. S. Raghavan and P. Raghavan, Hyperfine Interact. **9**, 317 (1981).